

Effects of Ferric Chloride on Structure, Surface Morphology and Combustion Property of Electrospun Polyacrylonitrile Composite Nanofibers

Yibing Cai^{1,2}, Dawei Gao¹, Qufu Wei^{1*}, Huili Gu¹, Shi Zhou¹, Fenglin Huang^{1**},
Lei Song², Yuan Hu², and Weidong Gao¹

¹Key Laboratory of Eco-textiles, Ministry of Education, Jiangnan University, Wuxi, 214122, Jiangsu, P.R. China

²State Key Laboratory of Fire Science, University of Science and Technology of China, Hefei, 230027, Anhui, P.R. China

(Received April 20, 2010; Revised August 26, 2010; Accepted September 4, 2010)

Abstract: In this work, the pure polyacrylonitrile (PAN) nanofibers and PAN/FeCl₃ composite nanofibers were prepared by an electrospinning process. Electrospinning solution properties including viscosity, surface tension and conductivity, had been measured and combined with the results of Scanning electron microscopy (SEM), Atomic force microscope (AFM) and Micro Combustion Calorimeter (MCC) to investigate the effects of FeCl₃ on the structure, surface morphology and combustion property of electrospun PAN nanofibers, respectively. It was found from SEM images that the diameters of composite nanofibers were decreased with the addition of FeCl₃, which was attributed predominantly to the increased conductivity of the polymer solutions compared to viscosity and surface tension. The AFM analyses revealed that the surface morphology of electrospun nanofibers changed from smooth and wrinkle-like structure (without FeCl₃) to rough and ridge-like structure (with FeCl₃). The results characterized by MCC showed that the loading of FeCl₃ decreased the heat release rate (HRR) and improved the combustion property of composite nanofibers.

Keywords: Electrospinning, PAN/FeCl₃ composite nanofibers, Structure, Surface morphology, Combustion property

Introduction

Polymer nanofibers have interesting properties which are the result of their extremely high ratio of surface to weight compared to the other conventional fibrous structures. These make nanofibers ideal for use in such applications as filtration, sensor, protective clothing, tissue engineering and functional materials, attributed to the light weight, small diameters, controllable pore structures and tight pore sizes [1-5]. Electrospinning is currently one of the most versatile and promising processes for producing continuous nanofibers for both fundamental and application-oriented research, due to its capability and feasibility in generating large quantities of nanofibers. In the electrospinning process, the thin polymer jet is ejected when the electrostatic force applied to the droplets of polymer solutions to overcome the liquid surface tension. The charged jet is elongated and accelerated by the electrostatic field, undergoing stretching, solvent evaporation and deposition on a substrate as a random fibrous web [3,4].

It is also noticed that the electrospinning method had been more and more often used to prepare polymer/inorganic composite nanofibers, due to the fact that such nanofibers allow a unique blend of properties, such as good mechanical strength and heat stability of inorganic materials, and excellent flexibility and moldability of polymers, while they still can maintain other functional properties of either constituent. The used inorganic includes montmorillonite

(MMT) [1-5], Ag [6], ZnCl₂ [7], Fe₃O₄ [8], ferric acetylacetonate (Fe(acac)₃) [9], TiO₂ [10] and SiO₂ [11,12], etc. Various researches [1-5] on the formation, structure, morphology and properties of electrospun polymer/clay composite nanofibers have been performed. The results showed that the clay layers were well dispersed inside the composite nanofibers and were oriented along the fiber direction. The incorporation of a few percent of clay into the nanofibers increased the mechanical, thermal stability and fire retardant properties, compared to the pure polymer nanofibers. Wang *et al.* [6] prepared the PAN/Ag composite nanofibrous film through in situ reduction of silver ions in N₂H₄OH aqueous solution. The Ag nanoparticles with average diameter of 10 nm were dispersed homogeneously in PAN nanofibrous film. The results revealed that PAN embedded Ag nanoparticles had been partly converted to graphite structure at room temperature, may be caused by the function of Ag nanoparticles as a catalyst for dehydrogenation of hydrocarbon compound. Zhang *et al.* [7] explored the electrospinning of PAN/ZnCl₂ composite nanofibers and the response of these nanofibers to H₂S. The ZnCl₂ in composite nanofibers reacted with H₂S to form ZnS crystals on the fiber surface. These results suggested that PAN/ZnCl₂ nanofibers were potential candidates in H₂S sensing and removal. Zhang *et al.* [8] studied the effects of solution concentration, applied electrical voltage, federate and the distance between the needle tip to the collector on the PAN composite nanofibers morphology. The results also indicated that the introduction of Fe₃O₄ nanoparticles had a significant effect on the crystallinity of PAN and a strong interaction between PAN and Fe₃O₄ nanoparticles. The Fe₃O₄ nanoparticles in the composite nanofibers became magnetically

*Corresponding author: qfwei@jiangnan.edu.cn

**Corresponding author: windhuang325@163.com

harder with a much larger coercivity than that of the dried nanoparticles. Wang *et al.* [9] prepared and investigated carbon nanofibers and C/Fe₃O₄ composite nanofibers by electrospinning of PAN-based nanofibers and subsequent carbonization processes. The addition of Fe₃O₄ in the composite played an important role in increasing the effective surface area, enhancing the electronic conductivity and improving the wettability of the electrode. These superior electrochemical properties of the composite nanofibers indicated that this unique composite may be a promising anode material for high performance lithium-ion batteries.

In the present work, we report the incorporation of ferric chloride (FeCl₃) into polymer nanofibers by electrospinning to form a new type of functional material. FeCl₃ is an important transition metal halide which is often used as Lewis acids. Lewis acids represent a wide range of chemical substances that are able to accept an electron pair and create a coordinate bond. It is known that some polymers with strongly electronegative groups (e.g., -CN) can coordinate Lewis acids and this may change the polymer degradation mechanism, and Lewis acid-type transition metal chlorides can also act as effective crosslinking catalysts [13-15]. The catalyzing effect of the Fe³⁺ would promote the cross-bonding of the polymer and form charred residue, which prevented the composite nanofibers from decomposing [16]. Meanwhile, the Fe³⁺ could capture the radicals during the thermal degradation of the composite nanofibers via gas-phase flame-retardant mechanism [17]. Current research efforts have focused on the effects of FeCl₃ on structure, surface morphology and combustion properties of the PAN composite nanofibers.

Experimental

Materials

The polyacrylonitrile (PAN, $M_w=79,100$) powder was obtained from Aldrich and used without further purification. The ferric chloride (FeCl₃·6H₂O) was obtained from the Shanghai Chemical Regents Company. The 99.5 % *N,N*-dimethyl formamide (DMF) was used as received. All chemicals were analytical grade and were used as received without further purification.

Preparation of Electrospinning Solutions

DMF solutions of PAN (12 wt%) containing various amount of FeCl₃ (0, 1, 3, and 5 wt%) were prepared at room temperature. Mechanical stirring was applied for at least 24 h to form homogeneous solutions.

Property Measurements of Electrospinning Solutions

The viscosity measurements were performed at room temperature in a Rotational Viscometer (NDJ-79). The surface tension of solutions was measured by a surface tension tensiometer (DSA100, KRUS Company) at room temperature,

and the solution conductivity was measured using a Digital Conductivity Meter (DDS-11A). Reproducibility of these solution properties was assessed by conducting all measurements on five samples.

Fabrication of Electrospun Composite Nanofibers

Electrospinning solutions were loaded in a 10 ml syringe with a stainless steel capillary metal-hub needle. The inner diameter of the metal needle was 0.30 mm. The positive electrode of the high voltage power supply was connected to the needle tip. The grounded electrode was connected to a metallic collector covered with an aluminum foil. The applied electrical voltage, working distance and federate were respectively fixed at 14 kV, 15 cm (the distance between the needle tip and the collection plate) and 0.4 ml/h. Under high voltage, a polymer jet was ejected and accelerated toward the counter electrode, during which the solvent was rapidly evaporated. Dry nanofibers were accumulated on the surface of aluminum foil and collected as a fibrous web.

Characterizations

Scanning electron microscope (SEM, SU-S3400) was used to examine the structures of the composite nanofibers. The samples were coated with a thin layer of gold by sputtering before the SEM imaging. An accelerating voltage of 15 kV with accounting time of 100 s was applied.

Atomic force microscope (AFM) was used to further observe the surface morphology of the composite nanofibers. The AFM used in this work was a Benyuan CSPM 4000. Scanning was carried out in tapping mode. All images were obtained at ambient conditions.

Combustion property was characterized by Micro Combustion Calorimeter (MCC) based on the principle of oxygen consumption. The signals from the MCC were recorded and analyzed by a computer system. The samples were firstly heated with a linear heating rate of 1 °C/s in pyrolyzed furnace. The decomposed products were brought away by inert gases, then were mixed with oxygen and came to the combustion chamber at 900 °C. Finally, the mixed gases were completely oxidated. The mass of samples for the MCC tests was about 4-6 mg.

Results and Discussion

Effects of Solution Properties on Composite Nanofibers

Figure 1 shows SEM images of electrospun PAN/FeCl₃ composite nanofibers from 12 wt% PAN solutions with different FeCl₃ concentrations (0, 1, 3, and 5 wt%) under the same conditions, such as fixed electrical voltage, federate and the distance between the needle tip to the collector. It was seen that all fibers were relatively uniform and randomly distributed to form the fibrous web, and beads or fibers with 'beads on a string' morphology [7] can seldom be found. It was also observed that the electrospun

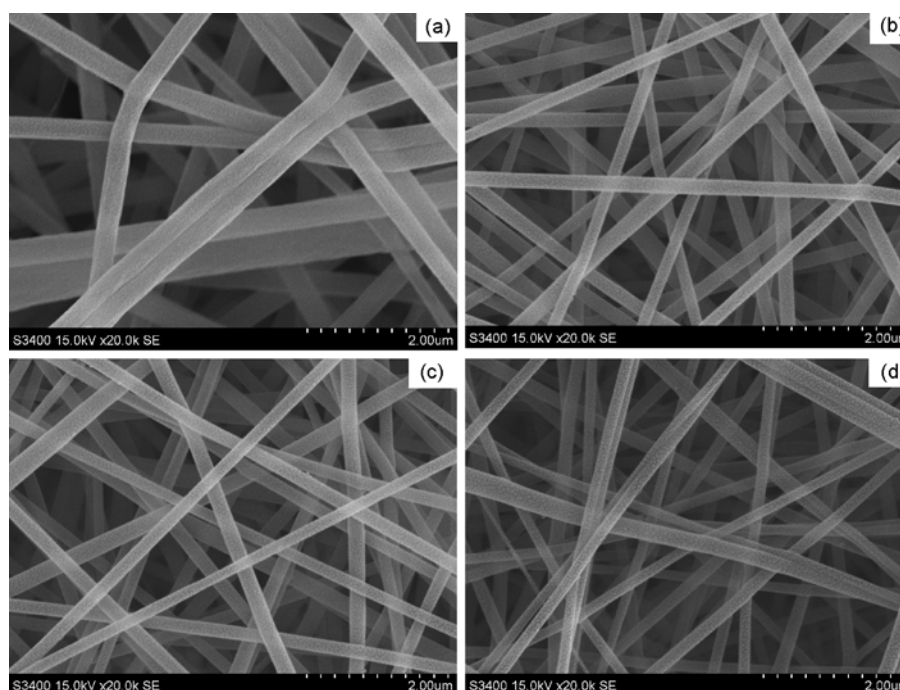


Figure 1. SEM images of the (a) PAN nanofibers, (b) PAN/1 wt% FeCl₃, (c) PAN/3 wt% FeCl₃, and (d) PAN/5 wt% FeCl₃ composite nanofibers.

nanofibers had variable fiber diameters. The morphology and average diameter of the electrospun PAN/FeCl₃ composite nanofibers were significantly affected by the loading of FeCl₃. The Figure 1(a) displayed that the average diameters of the PAN nanofibers were ranged from about 200 to 400 nm. However, the average diameters of the PAN/FeCl₃ composite nanofibers were decreased compared to those of the PAN nanofibers. The average diameter of electrospun PAN composite nanofibers with 1 wt% FeCl₃ was approximately 150-300 nm with better homogeneous distribution, as indicated in Figure 1(b). As showed in Figure 1(c), the average diameter of composite nanofibers was further decreased to 100-250 nm with an extremely homogeneous distribution, when the amount of the FeCl₃ increased to 3 wt%. When FeCl₃ concentration increased to 5 wt%, the average diameter of composite nanofibers decreased to about 50-200 nm. Meanwhile, the several nanofibers adhered together, could be also found in Figure 1(d). The average diameter of composite nanofibers was typically influenced by the viscosity, surface tension and conductivity of the electrospinning solution [7,8]. To understand the relationship between average diameter and FeCl₃ concentration, the viscosity, surface tension and conductivity were measured for all electrospinning solutions and were shown in Table 1. It could be found from Table 1 that there were slight increases in viscosity (e.g., an increase of 25.8 % when FeCl₃ concentration increased from 0 to 5 wt%) and surface tension (e.g., an increase of 17.0 % when FeCl₃ concentration

Table 1. Characteristics of PAN/FeCl₃ electrospinning polymer solutions

| FeCl ₃ (wt%) | Viscosity (mPaS) | Surface tension (mN/m) | Conductivity (μs/cm) |
|-------------------------|------------------|------------------------|----------------------|
| 0 | 575 | 215.78 | 84.6 |
| 1 | 650 | 245.01 | 117.1 |
| 3 | 750 | 251.18 | 134.2 |
| 5 | 775 | 259.81 | 149.3 |

increased from 0 to 5 wt%). The increases of viscosity and surface tension could be explained that the Lewis acids (FeCl₃) were able to create a coordinate bond with strongly electronegative groups (e.g., -CN) of the PAN [14,15]. The formed coordinate bonds increased molecular entanglement between PAN and FeCl₃. The polymer (PAN)-salt (FeCl₃)-solvent (DMF) interactions were likely another reason, and similar result could be also found in literature [8]. In addition, Table 1 also showed a dramatic influence of FeCl₃ on solution conductivity. Conductivity increased from 84.6 μs/cm (pure PAN) to 117.1 μs/cm (PAN/1 wt% FeCl₃), 134.2 μs/cm (PAN/3 wt% FeCl₃) and 149.3 μs/cm (PAN/5 wt% FeCl₃). The increase of conductivity reached 43.6 % for PAN/5 wt% FeCl₃ compared to the pure PAN, due to more free ions were available at higher FeCl₃ concentration. Moreover, the increased conductivity of the polymer solution increased the charge density in ejected jets and thus

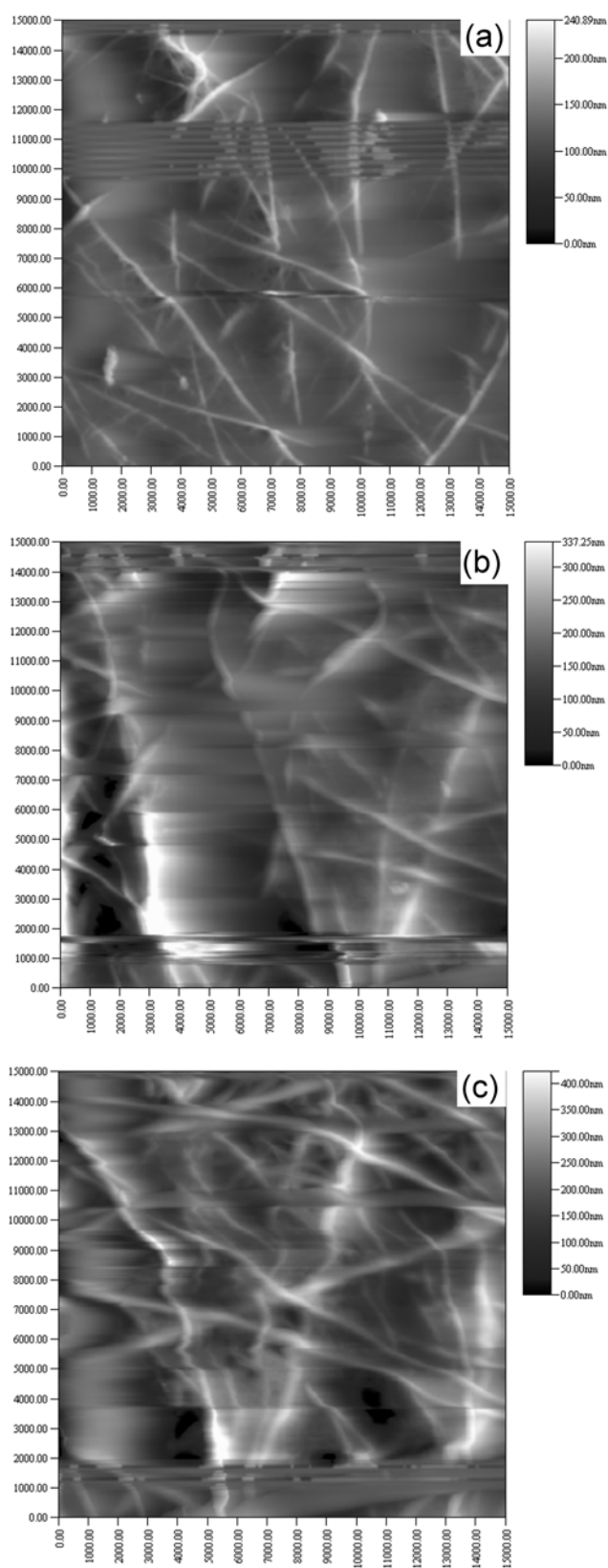


Figure 2. AFM images of (a) PAN nanofibers, (b) PAN/3 wt%FeCl₃, and (c) PAN/5 wt%FeCl₃ composite nanofibers.

stronger elongation forces were imposed to the jets because of the self-repulsion of the excess charges under the electrical field, resulting in substantially straighter shape and smaller diameter of electrospun fibers. This distinct change (an increase of 43.6 %) in solution conductivity was significantly greater than that of viscosity (25.8 %) and surface tension (17.0 %). Therefore, the decrease of nanofibers diameters with increasing FeCl₃ concentration should be attributed predominantly to the increased conductivity of the polymer solutions [7,8,16,18-20].

Surface Morphology

The surface morphology of electrospun nanofibers was investigated using AFM, which was shown in Figure 2. The three-dimensional fibrous webs consisted of many individual nanofibers with variable diameters, and the fibers were randomly oriented in the web. The pure PAN nanofibers showed a relatively smooth surface, with clear fibril structures of the fiber surface and a wrinkle-like morphology, as illustrated in Figure 2(a). This was attributed to the effects of drawing and high-shear flow during electrospinning. However, the PAN composite nanofibers with 3 wt% FeCl₃ were partly twisted, as indicated in Figure 2(b). Moreover, the twist changed to more observable with increasing addition of FeCl₃. The image in Figure 2(c) indicated that the surface of the electrospun composite nanofibers with 5 wt% FeCl₃ became rougher and formed a ridge-like morphology. The structure transformation of the nanofibers surface was mainly affected by the solvent vapor and conductivity behavior of the polymer solution. It was believed that a higher conductivity of the polymer solution resulted in more rapid or excessive solvent volatilization as the polymer jet traveled the distance from the needle tip to the metal target. In the electrospinning process, the addition of inorganic salt (FeCl₃) increased the charge density in ejected jets and thus stronger elongation forces were imposed to the jets because of the self-repulsion of the excess charges under the high electrical field. The electrical forces increased rapidly with the FeCl₃ loading and were far more the surface tensions of the solution under the same electrospinning conditions (fixed electrical voltage, working distance and federate), resulting in the ejected drops was accelerated. The speed of solvent volatilization increased with the acceleration of polymer jet during travel and led to the formation of twist structure and a rougher surface of the nanofibers.

Combustion Property

The Micro Combustion Calorimeter (MCC) was one of the most effective bench scale methods for investigating the combustion properties of polymer materials. The peak of heat release rate (PHRR) had been found to be one of the most important parameters to evaluate fire safety [21,22]. The effects of FeCl₃ on the combustion properties of the PAN composite nanofibers were evaluated by MCC in the

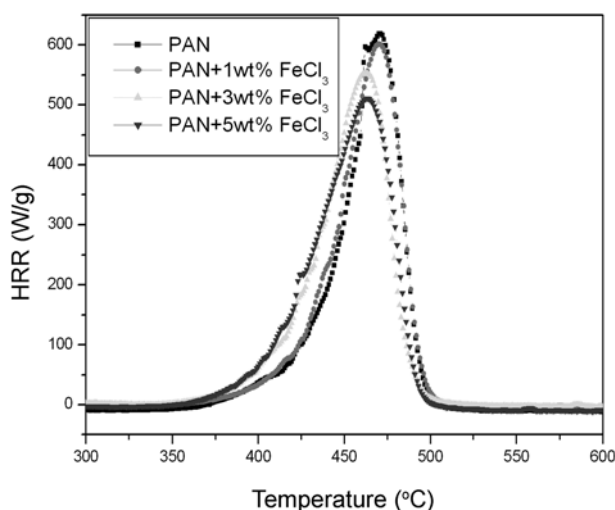


Figure 3. Heat release rate (HRR) curves of the PAN nanofibers and PAN/ FeCl_3 composite nanofibers.

present work and compared to the pure PAN nanofibers. The corresponding HRR curves were illustrated in Figure 3. The PHRR of the PAN/ FeCl_3 composite nanofibers decreased respectively to 601.3 W/g (PAN/1 wt% FeCl_3), 554.4 W/g (PAN/3 wt% FeCl_3) and 511.1 W/g (PAN/5 wt% FeCl_3) from 618.9 W/g for PAN nanofibers. The PHRR had respectively 2.84, 10.4, and 17.4 % decreases for PAN composite nanofibers with 1, 3, and 5 wt% FeCl_3 , compared with that of pure PAN nanofibers. The reasons may be that the transition metal chlorides delayed the escape of pyrolytic products and initiated the formation of macroradicals during combustion and thus led to radical recombination and intermolecular crosslinking [13-15]. It was also believed that the Fe ion could capture the radicals during the combustion of the composite nanofibers via gas-phase flame-retardant mechanism [17]. The decreased PHRR reduced combustion property of the PAN composite nanofibers.

It could be also found that the peak positions for the PAN composite nanofibers shifted to lower temperature, the times to reach the peak values of composite nanofibers were both relatively short in comparison with pure PAN nanofibers. Moreover, the initial HRR for the composite nanofibers were higher than that of the pure PAN nanofibers at the beginning of combustion. The reasons may be that the sublimation of FeCl_3 resulted in the formation of volatile combustibles in the early stages of composite nanofibers under at evaluated temperature. The second reason was probably the coordination of FeCl_3 to the electronegative cyano groups (-CN) of the PAN chains. The FeCl_3 could thermally lose a halogen atom through a reversible oxidative-reductive catalytic process between Fe^{3+} and Fe^{2+} during the combustion process [13,14]. This reaction should be accelerated by the additional coordination to the cyano (-CN) groups. Besides, the Lewis acid-type transition metal

chloride (FeCl_3) would also further catalyze the degradation of polymer matrixes [13,23-25]. Therefore, although the sublimation and catalysis effects of FeCl_3 led to the slight higher HRR during the initial combustion, the macroradicals recombination and intermolecular crosslinking induced by FeCl_3 and gas-phase flame-retardant mechanism decreased distinctly the PHRR of composite nanofibers, contributed to the improved combustion property.

Conclusion

In the present work, The PAN/ FeCl_3 composite nanofibers were prepared by a facile compounding and electrospinning. The effects of FeCl_3 with different amounts on structures, surface morphology and combustion properties of PAN composite nanofibers were respectively investigated by SEM, AFM and MCC. The SEM images showed that the average diameters of composite nanofibers decreased with the increasing FeCl_3 amounts, due predominantly to the increased conductivity of the polymer solutions compared to viscosity and surface tension. The AFM analyses indicated the formations of rough and ridge-like structures on the surface of PAN/ FeCl_3 composite nanofibers, and then smooth and wrinkle-like structures for the pure PAN nanofibers. It could be found from MCC tests that the addition of FeCl_3 induced the macroradicals recombination and intermolecular crosslinking via gas-phase flame-retardant mechanism, and decreased distinctly the PHRR, which contributed to the improved combustion property of composite nanofibers.

Acknowledgement

The work was financially supported by the National Natural Science Foundation of China (No. 51006046), the Natural Science Fund of Jiangsu Province (No. BK2010140), the Research Fund for the Doctoral Program of Higher Education of China (No. 200802951011 and No. 20090093110004), the Open Project Program of State Key Laboratory of Fire Science, University of Science and Technology of China (No. HZ2009-KF06), the Fundamental Research Funds for the Central Universities (No. JUSRP20903), the Natural Science Initial Research Fund of Jiangnan University (No. 2008LYY002), the Open Project Program of Key Laboratory of Eco-Textiles, Ministry of Education, Jiangnan University (No. KLET0909), and the Open Project Program of Key Laboratory of Green Processing and Functional Textile of New Textile Materials, Ministry of Education, Wuhan Textile University (No. GTKL2009004).

References

1. H. Fong, W. D. Liu, C. S. Wang, and R. A. Vaia, *Polymer*, **43**, 775 (2002).

2. J. H. Hong, E. H. Jeong, H. S. Lee, D. H. Baik, S. W. Seo, and J. H. Youk, *J. Polym. Sci. Pol. Phys.*, **43**, 3171 (2005).
3. M. Wang, A. J. Hsieh, and G. C. Rutledge, *Polymer*, **46**, 3407 (2005).
4. L. Li, L. M. Bellan, H. G. Craighead, and M. W. Frey, *Polymer*, **47**, 6208 (2006).
5. G. M. Kim, G. H. Michler, F. Ania, and F. J. Balta Calleja, *Polymer*, **48**, 4814 (2007).
6. Y. Z. Wang, Q. B. Yang, G. Y. Shan, C. Wang, J. S. Du, S. G. Wang, Y. X. Li, X. S. Chen, X. B. Jing, and Y. Wei, *Mater. Lett.*, **59**, 3046 (2005).
7. L. W. Ji, A. J. Medford, and X. W. Zhang, *Polymer*, **50**, 605 (2009).
8. D. Zhang, A. B. Karki, D. Rutman, D. P. Young, A. Wang, D. Cocke, T. H. Ho, and Z. H. Guo, *Polymer*, **50**, 4189 (2009).
9. L. Wang, Y. Yu, P. C. Chen, D. W. Zhang, and C. H. Chen, *J. Power Sources*, **183**, 717 (2008).
10. J. S. Im, M. I. Kim, and Y. S. Lee, *Mater. Lett.*, **62**, 3652 (2008).
11. L.W. Ji and X.W. Zhang, *Mater. Lett.*, **62**, 2161 (2008).
12. H. R. Jung, D. H. Ju, W. J. Lee, X. W. Zhang, and R. Kotek, *Electrochim. Acta*, **54**, 3630 (2009).
13. Y. B. Cai, Y. Hu, L. Song, S. Y. Xuan, Y. Zhang, Z. Y. Chen, and W. C. Fan, *Polym. Degrad. Stabil.*, **92**, 490 (2007).
14. J. W. Jang, J. H. Kim, and J. Y. Bae, *Polym. Degrad. Stabil.*, **88**, 324 (2005).
15. J. W. Jang, J. H. Kim, and J. Y. Bae, *Polym. Degrad. Stabil.*, **90**, 508 (2005).
16. Y. B. Cai, F. L. Huang, Q. F. Wei, L. Song, Y. Hu, Y. Ye, Y. Xu, and W. D. Gao, *Polym. Degrad. Stabil.*, **93**, 2180 (2008).
17. J. Zhu, F. M. Uhl, A. B. Morgan, and C. A. Wilkie, *Chem. Mater.*, **13**, 4649 (2001).
18. X. H. Zong, K. Kim, D. F. Fang, S. F. Ran, B. S. Hsiao, and B. Chu, *Polymer*, **43**, 4403 (2002).
19. W. K. Son, J. H. Youk, T. S. Lee, and W. H. Park, *Polymer*, **45**, 2959 (2004).
20. J. S. Choi, S. W. Lee, L. Jeong, S. H. Bae, B. C. Min, and J. H. Youk, *Int. J. Biol. Macromolecules*, **34**, 249 (2004).
21. H. Qiao, Y. B. Cai, F. Chen, Q. F. Wei, F. Q. Weng, F. L. Huang, L. Song, Y. Hu, and W. D. Gao, *Fiber. Polym.*, **10**, 750 (2009).
22. M. Zanetti, T. Kashiwagi, L. Falqui, and G. Camino, *Chem. Mater.*, **14**, 881 (2002).
23. J. T. Klopogge, *J. Porous Mat.*, **5**, 5 (1998).
24. Z. Ding, J. T. Klopogge, and R. L. Frost, *J. Porous Mat.*, **8**, 273 (2001).
25. J. Liu, Y. Hu, S. F. Wang, L. Song, Z. Y. Chen, and W. C. Fan, *Colloid. Polym. Sci.*, **282**, 291 (2004).